depth of the channel from the orifice. Secondly, here we encounter intense dissolution of the air trapped in the channel, and the rate at which this occurs substantially exceeds (in the case of water, by several orders of magnitude) the speed with which the solution is accomplished in a cylindrical capillary.

These results are important in the practice of capillary defectoscopy, pointing the way to finding optimum conditions for more complete and rapid filling of defects by means of tracer fluids.

LITERATURE CITED

1. G. A. Aksel'rud and M. A. Al'tshuler, Introduction to Capillary-Chemical Technology [in Russian], Moscow (1983).
2. N. P. Migun and P. P. Prokhorenko, Izv. Akad. Nauk BSSR, Ser. Fiz.-Tekh. Nauk, No. 3, 72-77 (1987).
3. P. P. Prokhorenko, M. S. Belyalov, N. V. Dezhkunov, and I. V. Stoicheva, Izv. Akad. Nauk BSSR, Ser. Fiz.-Tekh. Nauk, No. 2, 105-108 (1988).

NUMERICAL MODELING OF NONSTEADY NATURAL CONVECTION IN PRISMATIC CAVITIES

Yu. E. Karyakin

UDC 536.25

A finite-difference method is described for the calculation of the two-dimensional nonsteady natural convection in arbitrary areas. This method is used to investigate convection in a cavity of trapezoidal cross section.

One of the fundamental questions that arises in the numerical modeling of the processes of natural convection in cavities of arbitrary configuration is the choice of the coordinate system. The utilization of a rectangular Cartesian system involves certain difficulties in the formulation of the boundary conditions at irregular grid nodes and leads to a loss of accuracy in the solution. In a number of cases, it is possible to introduce mixed systems (rectangular Cartesian systems in rectilinear segments, and polar systems in those segments formed by circles, etc.). It is obvious that not every configuration of this region lends itself to this approach; moreover, difficulties arise in joining the solutions at the boundaries of the subregions.

The most effective coordinate system is the one in which the boundaries of the region being studied coincide with the coordinate lines. In the general case, this system will be curvilinear and nonorthogonal. It is precisely systems such as these that are examined in this paper.

Convection in prismatic cavities of nonrectangular lateral cross section has been investigated in [1-5]. The two-dimensional natural convection in a cavity whose lateral cross section is in the form of a parallelogram is examined in [1]. The vertical walls are assumed to be isothermal (hot and cold), and either a linear distribution of temperature or a condition of thermal insulation is specified for the remaining two parallel walls. The calculation results are compared with experimental data. The same authors, in [2], solved the problem in a conjugate formulation.

Convection in a trapezoidal region formed by the arcs of concentric circles and radial straight lines is examined in [3]. In [4], the authors investigate the problem experimentally. Finally, convection is modeled in [5] in a trapezoidal cavity with thermally insulated bases and walls that are isothermally inclined at an angle of 45° to the base. The numerical solution of the problem is found by utilizing variable stream functions, i.e., vorticity in a range of $10^2 \leq Ra \leq 10^5$ for various orientations of the cavity relative to the vector of the force of gravity.

Kalinin Polytechnic Institute, Leningrad. Translated from Inzhenerno-Fizicheskii Zhurnal, Vol. 56, No. 4, pp. 565-572, April, 1989. Original article submitted September 29, 1987.

0022-0841/89/5604-0397$12.50

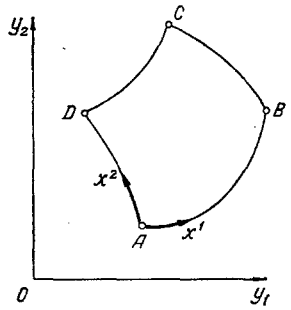

Fig. 1. The convection region.

Let us examine a prismatic cavity of rather great extent, whose lateral cross section is a quadrangle ABCD with arbitrary curvilinear boundaries (Fig. 1). The equations of the two-dimensional nonsteady natural convection in the Boussinesq approximation in the Cartesian coordinate system (y_1, y_2) have the form:

$$\frac{\partial u_i}{\partial t}+\frac{\partial}{\partial y_k}(u_k u_i)=-\mathrm{Gr}\frac{g_{yi}}{g}\theta-\frac{\partial p}{\partial y_i}+\frac{\partial}{\partial y_k}\left(\frac{\partial u_i}{\partial y_k}\right), \tag{1}$$

$$\frac{\partial \theta}{\partial t}+\frac{\partial}{\partial y_k}(u_k\theta)=\frac{1}{\mathrm{Pr}}\frac{\partial}{\partial y_k}\left(\frac{\partial \theta}{\partial y_k}\right), \tag{2}$$

$$\frac{\partial u_k}{\partial y_k}=0,\ i=1,\ 2;\ k=1,\ 2. \tag{3}$$

The twice-repeated subscripts here and below denote summation from 1 to 2.

Equations (1)-(3) have been written in dimensionless form. We have chosen some characteristic length L as the linear scale, and for the time scale we have taken the diffusion time $t_0 = L^2/\nu$, the velocity scale is $u_0 = L/t_0 = \nu/L$, and the pressure scale is the doubled dynamic thrust $\rho u_0^2 = \rho\nu^2/L^2$. In this case, the Prandtl number $\mathrm{Pr} = \rho\nu c_p/\lambda$, and the Grashof number $\mathrm{Gr} = \beta g(T_1 - T_2)L^3/\nu^2$, where T_1 and T_2 are characteristic values of temperature.

Let us introduce a curvilinear nonorthogonal system of coordinates $x^1 = x^1(y_1, y_2)$, $x^2 = x^2(y_1, y_2)$, representing the region of flow ABCD (Fig. 1) under consideration per square unit ($0 \le x^1 \le 1$, $0 \le x^2 \le 1$). In this system the tensor form of notation [6] corresponds to Eqs. (1)-(3):

$$\frac{\partial v_i}{\partial t}+\nabla_k(v^k v_i)=-\mathrm{Gr}\frac{g_i}{g}\theta-\nabla_i p+g^{kl}\nabla_k(\nabla_l v_i), \tag{4}$$

$$\frac{\partial \theta}{\partial t}+\nabla_k(v^k\theta)=\frac{1}{\mathrm{Pr}}g^{kl}\nabla_k(\nabla_l\theta), \tag{5}$$

$$g^{kl}\nabla_k v_l=0. \tag{6}$$

Let us present Eqs. (4)-(6) in a form which contains no tensor derivatives. For this we will use the familiar tensor-analysis formulas [6]:

$$v_i=u_\alpha\frac{\partial y_\alpha}{\partial x^i},\ v^i=u_\alpha\frac{\partial x^i}{\partial y_\alpha},\ u_i=v_\alpha\frac{\partial x^\alpha}{\partial y_i}=v^\alpha\frac{\partial y_i}{\partial x^\alpha}. \tag{7}$$

With utilization of (7) we can transform all of the tensor derivatives in (4)-(6). For example, the derivative $\nabla_k v_l$ is transformed in the manner of the twice-covariant rank-II tensor, i.e.,

$$\nabla_k v_l=\frac{\partial u_\alpha}{\partial y_\beta}\frac{\partial y_\beta}{\partial x^k}\frac{\partial y_\alpha}{\partial x^l}=\frac{\partial u_\alpha}{\partial x^k}\frac{\partial y_\alpha}{\partial x^l}=\frac{\partial \hat{v}_l}{\partial x^k},$$

where the symbol ($\hat{}$) denotes the quantities calculated on the basis of the Cartesian velocity-vector components with the aid of the derivative matrix $\partial y_\alpha/\partial x^l$, fixed at the differentiation point Q:

$$\hat{v}_l=u_\alpha(\partial y_\alpha/\partial x^l)_Q=v_k\partial x^k/\partial y_\alpha(\partial y_\alpha/\partial x^l)_Q.$$

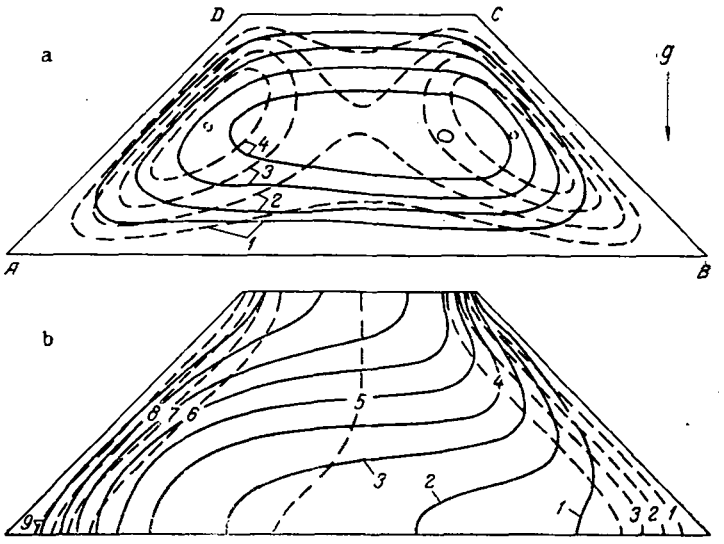

Fig. 2

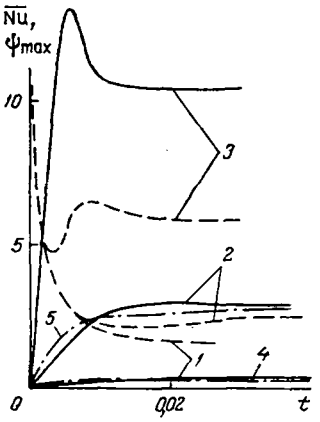

Fig. 3

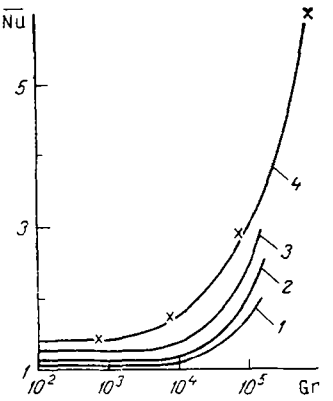

Fig. 4

Fig. 2. Streamlines (a) and isotherms (b) in a trapezoidal cavity; Gr = $7.4 \cdot 10^5$, $\varphi = 45°$; dashed lines) t = $9.4 \cdot 10^{-4}$; solid lines) steady-state regime.

Fig. 3. The function $\psi_{max}(t)$ (the solid and dash–dot curves) and $\overline{Nu}(t)$ (dashed curves) for a trapezoidal cavity, $\varphi = 45°$: 1) Gr = $7.4 \cdot 10^3$; 2) $7.4 \cdot 10^4$; 3) $7.4 \cdot 10^5$; $\varphi = 15°$; 4) Gr = 10^4; 5) 10^5.

Fig. 4. The effect exerted by the angle of inclination of the side wall of the trapezoidal cavity on the function $\overline{Nu}(Gr)$: 1) $\varphi = 0$; 2) 15; 3) 30; 4) 45°; the points identify the data from [5] for $\varphi = 45°$.

As a consequence of such transformations the system of equations (4)-(6) is reduced to the following form [7-9]:

$$\frac{\partial v_i}{\partial t} + \frac{\partial (\hat{v}^k \hat{v}_i)}{\partial x^k} = -\mathrm{Gr}\,\frac{g_i}{g}\,\theta - \frac{\partial p}{\partial x^i} + \frac{\partial}{\partial x^k}\left(\hat{g}^{kl}\,\frac{\partial \hat{v}_i}{\partial x^l}\right), \tag{8}$$

$$\frac{\partial \theta}{\partial t} + \frac{\partial (\hat{v}^k \theta)}{\partial x^k} = \frac{1}{\mathrm{Pr}}\,\frac{\partial}{\partial x^k}\left(\hat{g}^k{}_l\,\frac{\partial \theta}{\partial x^l}\right), \tag{9}$$

$$g^{kl}\,\frac{\partial \hat{v}_l}{\partial x^k} = 0, \quad i, k, l = 1, 2, \tag{10}$$

where

$$\hat{v}^k = u_\alpha \left(\frac{\partial x^k}{\partial y_\alpha}\right)_Q;\ \hat{g}^{kl} = \left(\frac{\partial x^k}{\partial y_\alpha}\right)_Q \frac{\partial x^l}{\partial y_\alpha}.$$

The system of equations (8)-(10) describes the nonsteady natural convection in an arbitrary two-dimensional region ABCD (Fig. 1) and must be enhanced with the appropriate conditions for all the solid boundaries: adhesion and impermeability for the I-st or II-nd kind of velocity-vector components with temperature θ.

Since the pressure p in the solution of the problem in physical variables is determined with accuracy to the additive constant, we make use of the additional condition: $p = 0$ at the point $x^1 = x^2 = 0$. No other pressure-related boundary conditions are imposed.

For purposes of constructing the difference scheme, in the integration region ($0 \le x^1 \le 1$, $0 \le x^2 \le 1$) we will employ the nonuniform grid $x^1 = x_n{}^1$ ($n = 1, 2, \ldots, N + 1$), $x^2 = x_m{}^2$ ($m = 1, 2, \ldots, M + 1$). Let us introduce variable intervals along the coordinates x^1 and x^2 with exponential constrictions near the solid boundaries. For this purpose we will consider the auxiliary variable η which, in this grid, has a constant interval $\Delta\eta$ which is associated, for example, with the coordinate x^1 by the relationship

$$\eta = \frac{1}{2}\left[1 + \frac{\ln(1 + d_1 x^1)}{\ln(1 + d_1)} - \frac{\ln(1 + d_2(1 - x^1))}{\ln(1 + d_2)}\right],$$

where $0 \le \eta \le 1$. In the calculations it was generally assumed that $d_1 = d_2 = 10$.

Let us determine the unknown grid functions p and θ at the center of each grid cell, and let us also determine the functions v_1 and v_2 at the center of its boundaries, as this is done in the marker and cell method [10]. We will use D_k to denote the approximation of the derivative $\partial/\partial x^k$ with respect to the adjacent nodes. The convection terms in Eqs. (8) and (9) will be approximated in accordance with the donor cell scheme [10], denoting the difference analog of the derivative $\partial(\hat{v}^k\Phi)/\partial x^k$ by $D_k{}^*(\hat{v}^k, \Phi)$, where $\Phi = \hat{v}_i, \theta$.

We will use the following multiple-interval semiimplicit difference scheme [9] to solve system of equations (8)-(10) (the superscript n identifies the number of the time layer):

$$\delta v_i/\Delta t + D_k^*(\hat{v}^{kn}, \hat{v}_i^n) = -\mathrm{Gr} g_i g^{-1}\theta^n - D_i(p^n) + D_k(\hat{g}^{kl} D_l(\hat{v}_i^n)), \tag{11}$$

$$g^{kl} D_k(\hat{v}_l^n + \delta\hat{v}_l - \Delta t \cdot \hat{g}_l^j D_j(\delta p)) = 0, \tag{12}$$

$$v_i^{n+1} = v_i^n + \delta v_i - \Delta t \cdot D_i(\delta p), \tag{13}$$

$$\delta\theta/\Delta t + D_k^*(\hat{v}^{k\,n+1}, \theta^n) = \mathrm{Pr}^{-1} \cdot D_k(\hat{g}^{kl} D_l(\theta^n)), \tag{14}$$

$$\theta^{n+1} = \theta^n + \delta\theta,\ p^{n+1} = p^n + \delta p, \tag{15}$$

where

$$\hat{g}_l^j = \frac{\partial x^j}{\partial y_k}\left(\frac{\partial y_k}{\partial x^l}\right)_Q,\ \delta\hat{v}_i = \delta v_k \cdot \hat{g}_i^k.$$

The procedure for the realization of the difference scheme (11)-(15) is as follows. From the known values of the grid functions $v_1{}^n$, $v_2{}^n$, p^n, and θ^n on the n-th time layer, by means of the explicit expressions (11) we calculate the correction factors for the velocities δv_1 and δv_2. Then, in conjunction with Eq. (12), on the basis of the implicit scheme, iterations are used to find the field of correction factors for the pressure δp, subsequent to which, from expression (13), we determine the values of the grid functions $v_1{}^{n+1}$, $v_2{}^{n+1}$ on the new (n + 1)-th time layer. Finally, on the basis of the explicit procedure (14) we calculate the field of correction factors for the temperature $\delta\theta$, and from expressions (15), by means of simple recalculation, we find the sought grid functions θ^{n+1} and p^{n+1} on the (n + 1)-th time layer.

For the purpose of finding the field correction factors for the pressure δp, a term with the derivative with respect to the relaxation time $\partial(\delta p)/\partial\tau$ is added to Eq. (12), which is then solved by a three-dimensional variable iteration decomposition scheme (s is the iteration number) [9]:

$$\xi^{s+1/2}/\Delta\tau - \alpha g^{11} D_1 D_1 (\xi^{s+1/2}) - g^{kl} D_k (\hat{g}_l^{\beta} D_{\beta} (\delta p^s)) + g^{kl} \Delta t^{-1} D_k (\hat{v}_l^n + \delta \hat{v}_l^{n+1/2}) = 0, \tag{16}$$

$$(\xi^{s+1} - \xi^{s+1/2})/\Delta\tau - \alpha g^{22} D_2 D_2 (\xi^{s+1}) = 0, \tag{17}$$

$$\delta p^{s+1} = \delta p^s + \xi^{s+1}. \tag{18}$$

Scheme (16)-(18) is realized by successive scalar sweeps along the directions of x^1 and x^2. To speed up the convergence of the iteration process, we use a set of relaxation-time intervals $\Delta\tau\{\Delta\tau_0, \Delta\tau_1, \ldots, \Delta\tau_R\}$, which ensures uniform attenuation of the harmonic perturbation over the entire spectrum of eigenfrequencies in the problem [9]. Analysis of the model equation with constant coefficients shows that for an arbitrary curvilinear coordinate system the interval sequence can be ascertained with the following formulas:

$$q = \min(\pi\Delta x^1/4,\ \pi\Delta x^2/4)^{2/R},$$
$$\Delta\tau_0 = \min[(\Delta x^1)^2/(4\alpha g^{11}),\ (\Delta x^2)^2/(4\alpha g^{22})],$$
$$\Delta\tau_r = \Delta\tau_{r-1}/q,\ r = 1, 2, \ldots, R.$$

As was demonstrated by these calculations, in the first time layer the algorithm from (16)-(18) calls for the completion of approximately 20 iterations; however, the number of iterations for the following time layers rapidly diminishes to a minimum value s = R + 1. It was generally assumed that R = 3-5.

We note that system (16)-(18) requires no formulation of boundary conditions for pressure correction factors. The difference analogs of the differential operators near the boundaries of the region are written so that only the boundary conditions for the velocity vector and temperature vector components are used [11]. In setting the temperature conditions of the II-nd kind we should take into consideration that the derivative with respect to the normal to the coordinate line x^1 = const has the form

$$\left.\frac{\partial\theta}{\partial n}\right|_{x^1=\text{const}} = \frac{1}{\sqrt{g^{11}}}\left(g^{11}\frac{\partial\theta}{\partial x^1} + g^{21}\frac{\partial\theta}{\partial x^2}\right), \tag{19}$$

while with respect to the normal to the line x^2 = const

$$\left.\frac{\partial\theta}{\partial n}\right|_{x^2=\text{const}} = \frac{1}{\sqrt{g^{22}}}\left(g^{12}\frac{\partial\theta}{\partial x^1} + g^{22}\frac{\partial\theta}{\partial x^2}\right). \tag{20}$$

Expressions (19) and (20) simultaneously include the derivatives $\partial\theta/\partial x^1$ and $\partial\theta/\partial x^2$. Consequently, at that boundary where the temperature condition of the II-nd kind is given, its difference analog can be realized with utilization of the sweeping method along this boundary.

The above-described algorithm was used to calculate the two-dimensional nonsteady natural convection in a prismatic cavity whose lateral cross section is an equilateral trapezoid (Fig. 2) with a base length L and height H. The sides form an angle φ with the vertical.

We will introduce the curvilinear coordinate system (x^1, x^2) in the following fashion:

$$x^1 = \frac{y_1 - y_2\operatorname{tg}\varphi}{L - 2y_2\operatorname{tg}\varphi},\ x^2 = \frac{y_2}{H}. \tag{21}$$

Here, the trapezoidal region of motion in the (y_1, y_2) coordinate plane is transformed to the quadratic in the (x^1, x^2) plane, so that $0 \le x^1, x^2 \le 1$, while the boundaries of the region coincide with the coordinate lines x^1 = const, x^2 = const.

Using (21) and the reciprocal transformations of the coordinates, we can easily find the values of the matrix elements needed for the calculations of the derivatives $\partial y_\alpha/\partial x^i$ and $\partial x^i/\partial y_\alpha$ (i, α = 1, 2).

We will assume that the upper and lower bases of the cavity have been thermally insulated, and that the side surfaces are isothermal: the left-hand side AD is the hot side, while the right-hand side BC is the cold side (Fig. 2), i.e.,

$$\left.\frac{\partial\theta}{\partial n}\right|_{AB} = \left.\frac{\partial\theta}{\partial n}\right|_{DC} = 0,\ \theta_{AD} = 1,\ \theta_{BC} = 0.$$

In the solution of the nonsteady problem it is assumed that at the initial instant of time the liquid is nonmoving throughout the entire convection region and that its temperature throughout is equal to $\theta_{init} = 0.5$.

Systematic calculations were performed over a Grashof number range $10^2 \leq Gr \leq 10^6$ for four values of the angle at which the side walls deviate from the vertical: $\varphi = 0$, 15, 30, and 45°. It was assumed that L = 1, H = L/3, and Pr = 0.7.

Within the indicated range of parameters we have constructed time-developed streamline patterns, as well as those of the isotherms, and the maximum values of the stream function whose magnitude in the section $x^1 = \text{const}$ is determined on the basis of the expression

$$\psi = \int_0^{x^2} \sqrt{g_{22}/g^{11}}\,(v_1 g^{11} + v_2 g^{21})\,dx^2,$$

as well as the distributions of the Nusselt numbers at the side walls of the cavity: $Nu = (\partial\theta/\partial n)_w$. These results have been compared with the data from [5].

The solid lines in Fig. 3 show the change over time in the maximum value of the stream function in the cavity for the case in which $\varphi = 45°$ and for three values of the Grashof number: $7.4 \cdot 10^3$, $7.4 \cdot 10^4$, and $7.4 \cdot 10^5$ (with consideration of the difference in the choice of scales, this corresponds to $Ra = 10^3$, 10^4, and 10^5 from [5]), as well as the values of the average Nusselt number at the side wall of the cavity for these cases.

With comparatively small Grashof numbers, $Gr \leq 10^4$, the maximum value of the stream function, characterizing the intensity of convective motion, increases monotonically over time, attaining some limit. The values of the average Nu numbers are large at the beginning of the convection process because of the large temperature gradients near the walls; subsequently, they diminish monotonically over time, tending to some limit.

If $Gr > 10^4$, the functions $\psi_{max}(t)$ and $\overline{Nu}(t)$ no longer exhibit a monotonic nature. At some instant of time the quantity ψ_{max} reaches a maximum, and then, diminishing, tends to a steady-state value. The nonmonotonic behavior of the functions $\psi_{max}(t)$ and $\overline{Nu}(t)$ is also characteristic of other types of cavities. Thus, an analogous phenomenon has been described in [12] for the case of a triangular cavity.

The dash–dot lines in Fig. 3 are plots of the function $\psi_{max}(t)$ for $\varphi = 15°$ and for two values of the Gr number: 10^4 and 10^5. As we can see, with a reduction in the angle φ the intensity of the convection process within the cavity diminishes.

Figure 2 shows the development, over time, of the streamline patterns and those of the isotherms in the trapezoidal cavity. The dashed lines correspond to the initial stage of the convection, while the solid lines represent the steady-state regime. As follows from the figure, at the onset of the convection process, near the side walls, two circulation zones are formed and the direction of liquid rotation is clockwise. With the passage of time, these zones merge into a single circulation region. The isotherms in the central portion of the cavity assume a virtually horizontal position, corresponding to the conditions of liquid stratification.

Figure 4 shows the change in $\overline{Nu}(Gr)$ for various values of the angle φ, representing the deviation of the side walls from the vertical. As we can see, as the angle φ becomes larger, the intensity of the heat-exchange processes at the walls of the cavity increases noticeably.

All the calculations have been carried out on a nonuniform grid 30 × 30.

NOTATION

y_1, y_2, Cartesian coordinates; x^1, x^2, curvilinear coordinates; u_1, u_2, Cartesian velocity components; v_1, v_2 and v^1, v^2, covariant and contravariant velocity components; t, time; p, pressure; T, temperature; $\theta = (T - T_2)/(T_1 - T_2)$, the dimensionless temperature; $g^{k\ell}$, the contravariant components of the metric tensor; g_{22}, the twice-covariant component of the metric tensor; ∇_k, the symbol for the covariant derivative; ν, the kinematic coefficient of viscosity; ρ, the density of the working fluid; λ, the coefficient of thermal conductivity; β, the thermal coefficient of volume expansion; c_p, the coefficient of heat capacity; η, an auxiliary variable; d_1, d_2, the parameters of grid density; δv_i, $\delta\theta$, δp, the correction factors for the sought values of the velocity, temperature, and pressure components; $\Delta\tau$, the

relaxation-time interval; α, the weight coefficient; H, the height of the cavity; L, the width of the cavity; φ, the angle formed between the vertical and the side surface of the trapezoidal cavity; n, the coordinate of the orthogonal surface; ψ, the stream function; Gr, the Grashof number; Pr, the Prandtl number; Nu, the Nusselt number; Ra, the Rayleigh number; g, the acceleration of free fall; g_{yi}, the projection of g onto the y_i axis; g_i, the covariant component of the vector g.

LITERATURE CITED

1. H. Nakamura and Y. Asako, Bull. JSME, 23, No. 185, 1827-1834 (1980).
2. Y. Asako and H. Nakamura, Bull. JSME, 27, No. 228, 1144-1151 (1984).
3. Iikan, Bayazitoglu, and Witt, Teploperedacha, No. 4, 61-69 (1980).
4. Iikan, Witt, and Bayazitoglu, Teploperedacha, No. 4, 69-74 (1980).
5. T. S. Lee, Int. J. Heat Fluid Flow, 5, No. 1, 29-36 (1984).
6. N. E. Kochin, Vector Calculus and the Beginning of Tensor Calculus [in Russian], Moscow (1965).
7. V. E. Karyakin and Yu. E. Karyakin, "The dynamics of nonuniform and compressible media," Gazodinamika i teploobmen (Leningrad), No. 8, 112-121 (1984).
8. V. E. Karyakin and Yu. E. Karyakin, The Physics of Flowing Gas Discharge Systems [in Russian], ITMO AN BSSR, Minsk (1986), pp. 131-139.
9. V. E. Karyakin and Yu. E. Karyakin, Chislennye Metody Mekh. Sploshnoi Sredy, 17, No. 5, 91-100 (1986).
10. P. J. Roache, Computational Fluid Dynamics, Hermosa, Albuquerque, New Mexico (1976).
11. Yu. E. Karyakin, Chislennye Metody Mekh. Sploshnoi Sredy, 16, No. 3, 56-67 (1985).
12. Yu. E. Karyakin and Yu. A. Sokovishin, Izv. Akad. Nauk SSSR, Mekh. Zhidk. Gaza, No. 5, 169-173 (1985).

RELATIONSHIP BETWEEN THE COEFFICIENT OF MASS TRANSFER AND LOCAL EFFICIENCY FOR VAPOR (GAS)–LIQUID SYSTEMS

Yu. A. Komissarov, V. V. Kafarov, and K. Amirov

UDC 66.048.37

Using typical mathematical vapor and liquid models, we demonstrate analytically that the structure of the liquid flow in two-phase systems has no effect on the volumetric coefficient of mass transfer.

As we calculate the number of contact devices in rectification and absorption columns, the process of mass transfer is described by equations linking the efficiency of the plate with the parameters of the vapor–liquid flow model [1-3]. The magnitude of the local efficiency included in these equations, in its physical sense, characterizes the kinetics of mass transfer and it is determined in various ways [4-8]. The local efficiency is determined in [4, 5] from the equation which links this quantity with the number of transfer units, which, in its own turn, is calculated on the basis of a two-film mass-transfer model which involves the utilization of empirical relationships for the coefficients of mass transfer in the vapor and liquid phases. For purposes of calculating the local efficiency, the theoretical and experimental liquid-concentration profiles are compared in [6] over the length of the plate during the mass-transfer process (adsorption), while regime and technological parameters for an operational rectification column are used in [7, 8]. The algorithm used to calculate the local efficiency makes provision for reducing to a minimum the mean-square error in the theoretical and experimental concentration profiles [6] or to find the optimum magnitudes of the local component efficiency in such a manner that the theoretical and actual

Mendeleev Chemical Technology Institute, Moscow.

Translated from Inzhenerno-Fizicheskii Zhurnal, Vol. 56, No. 4, pp. 572-580, April, 1989. Original article submitted May 5, 1987.

0022-0841/89/5604-0403$12.50